CdSe Nano-tetrapods: Controllable Synthesis, Structure Analysis, and Electronic and Optical Properties

Qi Pang,[†] Lijuan Zhao,[†] Yuan Cai,[†] Duc Phuong Nguyen,[‡] Nicolas Regnault,[‡] Ning Wang,[†] Shihe Yang,[§] Weikun Ge,[†] Robson Ferreira,[‡] Gerald Bastard,[‡] and Jiannong Wang*[,†]

Physics Department and Chemistry Department, Hong Kong University of Science and Technology, Clear Water Bay, Hong Kong, China, and Laboratoire Pierre Aigrain, Ecole Normale Supérieure, 24 rue Lhomond F75005, Paris, France

Received April 12, 2005. Revised Manuscript Received August 8, 2005

Tetrapod-shaped CdSe nanocrystals have been successfully synthesized in high yields using a simple method of controlling the protonic acidity of the reaction system. A possible growth mechanism is discussed on the basis of the surface modification of H^+ present. The crystal structure of CdSe tetrapods is determined by high-resolution transmission electron microscopy analysis to have a zinc blende core at the center with four wurtzite arms growing out from the core along four [111] directions. The electronic structure of CdSe tetrapods is studied theoretically in comparison with that of spherical dots.

Introduction

The size and shape of semiconductor nanocrystals play an important role that determines their electronic and optical properties. During the past few years much effort has been devoted to controlling the size and shape of these materials. One way to achieve shape control is to enhance anisotropic nanocrystal growth using a liquid medium such as the vapor−liquid−solid (VLS) method.[1] Another common approach is to use surfactants or micelles (regular or inverse) as regulating agents or templates to facilitate anisotropic crystal growth.[2−6] The tetrapod-shaped nanocrystals can potentially lead to a variety of interesting mechanical, electrical, and optical properties. For example, due to their three-dimensional character, tetrapods may be important alternatives to fibers and rods as additives for mechanical reinforcement of polymers.[7] Tetrapods can also serve as a very interesting building block for preparing superstructures, especially three-dimensional ones.[8] Three-dimensional CdSe tetrapods have obvious potential advantages in photovoltaic devices[9,10] because their shape makes it impossible for them to lie flat within the film. Up to now tetrapod-shaped crystals with dimensions on the nanometer and micrometer scale have been synthesized for a variety of II−VI semiconductors including ZnO,[11−12] CdS,[13−15] CdTe,[7,16] and CdSe.[2,17] CdTe tetrapod-shaped nanocrystals have previously been synthesized using CdO as the cadmium precursor in oleic acid (OA)−trioctylphosphine (TOP) system or in a mixture of surfactant of octadecylphosphinic acid (ODPA) and the trioctylphosphine oxide (TOPO)−TOP system, respectively. It is found that it is possible to obtain a high yield of colloidal CdTe tetrapods with well-controlled nanoscale dimensions. On the other hand, only very low yield of colloidal CdSe tetrapods is observed in the synthesis of CdSe nanorods using CdO as the cadmium precursor in a mixture surfactant of tetradecylphosphonic acid (TDPA) and the TOPO−TOP system. In this paper, we report the syntheses of almost pure tetrapod-shaped CdSe nanocrystals using a simple method by controlling the protonic acidity of the cadmium OA−TOP precursor. The crystal structure of the tetrapods is determined by high-resolution transmission electron microscopy (HRTEM) analysis, which shows that the tetrapod has a zinc blende core and four wurtzite arms. The electronic structure of the tetrapod is calculated in comparison with the spherical dot. Room-temperature optical absorption spectra and photoluminescence (PL) spectra are measured.

Experimental Section

The syntheses of CdSe nanocrystals were carried out by standard air-free techniques. A mixture of CdO (1.8 mmol, 0.2311 g), oleic acid (OA, 6.0 mmol), and diphenyl ether (8 mL) was heated in a

* Corresponding author. E-mail: phjwang@ust.hk.
[†] Physics Department, Hong Kong University of Science and Technology.
[‡] Ecole Normale Supérieure.
[§] Chemistry Department, Hong Kong University of Science and Technology.

(1) Wu, Y.; Yang, P. *J. Am. Chem. Soc.* **2001**, *123*, 3165.
(2) Peng, A.; Peng, X. G. *J. Am. Chem. Soc.* **2002**, *124*, 3343.
(3) Yu, Y. Y.; Chang, S. S.; Lee, C. L.; Wang, C. R. C. *J. Phys. Chem. B* **1997**, *101*, 6661.
(4) Li, M.; Schnablegger, H.; Mann, S. *Nature* **1999**, *402*, 394.
(5) Puntes, V. F.; Krishnan, K. M.; Alivisatos, A. P. *Science* **2001**, *291*, 2115.
(6) Milliron, D. J.; Hughes, S. M.; Cui, Y.; Manna, L.; Li, J. B.; Wang, L. W.; Alivisatos, A. P. *Nature* **2004**, *430*, 190.
(7) Manna, L.; Milliron, D. J.; Meisel, A.; Scher, E. C.; Alivisatos, A. P. *Nat. Mater.* **2003**, *2*, 382.
(8) Liu, H. T.; Alivisatos, A. P. *Nano Lett.* **2004**, *4*, 2397.
(9) Sun, B. Q.; Marx, E.; Greenham, N. C. *Nano Lett.* **2003**, *3*, 961.
(10) Scher, E. C.; Manna, L.; Alivisatos, A. P. *Philos. Trans. R. Soc. London, Ser. A* **2003**, *361*, 241.
(11) Dai, Y.; Zhang, Y.; Li, Q. K.; Nan, C. W. *Chem. Phys. Lett.* **2002**, *83−86*, 358.
(12) Yan, H. Q.; He, R.; Pham, J.; Yang, P. D. *Adv. Mater.* **2003**, *15*, 402.
(13) Jun, Y. W.; Lee, S. M.; Kang, N. J.; Cheon, J. *J. Am. Chem. Soc.* **2001**, *123*, 5150.
(14) Jun, Y. W.; Jung, Y. Y.; Cheon, J. *J. Am. Chem. Soc.* **2002**, *124*, 615.
(15) Chen, M.; Xie, Y.; Lu, J.; Xiong, Y. J.; Zhang, S. Y.; Qian, Y. T.; Liu, X. M. *J. Mater. Chem.* **2002**, *12*, 748.
(16) Yu, W. W.; Wang, Y. A.; Peng, X. G. *Chem. Mater.* **2003**, *15*, 4300.
(17) Manna, L.; Scher, E. C.; Alivisatos, A. P. *J. Am. Chem. Soc.* **2000**, *122*, 12700.

10.1021/cm050774k CCC: $30.25
Published on Web 09/21/2005

three-neck flask to 180 °C for 2 h. Then 3.2 g of selenium−TOP solution (containing 0.32 g (4.0 mmol) of selenium) was quickly injected into this hot solution. The synthesis was carried out under N_2 flow. An aliquot at a given reaction time was taken out from the reaction flask with a small syringe and quickly transferred into a vial with chloroform. The rapid cooling of the hot aliquot by the cold chloroform sufficiently quenched the growth of the nanocrystals. The CdSe nanocrystal obtained in this way has spherical shape and is named as sample A. More importantly, we found that a CdSe nanocrystal with a tetrapod shape could be obtained by following the same procedure as described above except adding 0.2, 0.6, and 1.0 mmol HCl (37% aqueous solution), 0.2 mmol $MnCl_2$, $FeCl_2$, and H_2SO_4, respectively, to the mixture of CdO, OA, and diphenyl ether before heating. The samples obtained by separately adding HCl with different amounts of 0.2, 0.6, and 1.0 mmol are named as samples B1, B2, and B3, respectively. The samples obtained by separately adding $MnCl_2$, $FeCl_2$, and H_2SO_4 are named as samples C−E, respectively. When we monitor the growth of the tetrapods, we find that the solution becomes red colored immediately after Se−TOP solution is injected into the hot cadmium precursor with or without the addition of HCl, $MnCl_2$, $FeCl_2$, and H_2SO_4. This indicates the growth of quantum dots or tetrapods is very fast. However, the above-named samples are obtained with the reaction time of 1 h.

The size, shape, and crystal structures of CdSe nanocrystals were examined using a JEOL 2010F high-resolution transmission electron microscopy (HRTEM) operated at 200 kV with a spatial resolution of 0.17 nm. The compositions of CdSe nanocrystals were determined by X-ray energy dispersive spectrometry (EDS) in the TEM. UV/vis absorption spectra were obtained using a Milton Roy Spectronic 300 spectrometer. PL spectra were measured using a standard setup with argon laser ($\lambda = 488$ nm). For both optical absorption and PL experiments CdSe samples in solution were used.

Results and Discussions

Figure 1a shows a typical TEM image of dot-shaped CdSe nanocrystals, sample A. As can be seen, the CdSe quantum dots (QDs) are almost spherical, and the average size of the QDs is about 4 nm (estimated by averaging over 50 dots clearly visible in TEM pictures). Figure 1b is a low-magnification TEM image illustrating high yields of tetrapod-shaped CdSe nanocrystals (sample B2) formed by adding 0.6 mmol of HCl (37% aqueous solution) into cadmium precursor of the pure dot-shaped CdSe reaction system. It is estimated from a few such TEM images that the tetrapod yield is up to 80% for this sample, which is much higher than that previously reported.[2,17] Panels c−f of Figure 1 are typical TEM images showing tetrapod-shaped CdSe nanocrystals formed by adding 1.0 mmol of HCl (sample B3), 0.2 mmol of $MnCl_2$ (sample C), 0.2 mmol of $FeCl_2$ (sample D), and 0.2 mmol of H_2SO_4 (sample E), respectively, into cadmium precursor of the pure dot-shaped CdSe reaction system. The diameter of the core and the diameter and the length of the arms for some samples are estimated by HRTEM analysis. The results are listed in Table 1. The diameters of the core for all of the samples are about 4.1 nm, the widths of the arms are about 3.1 nm, and the lengths of the arms are about 8.3 nm. We have tried to vary the geometric shape of the tetrapod by changing the H^+ concentration from 10%, 30% to 50%, but no obvious differences are observed so far. In addition, by sampling aliquots of the reaction mixtures at 15 min, 30 min, and 1 h for analysis, respectively, we find that all of the samples show a high yield of tetrapods of similar geometrical sizes. The reason for no pronounced influence of the reaction time on the sizes of the tetrapods is as follows. The growths of tetrapods are so fast that the tetrapods with a narrow size distribution have been formed in 15 min. The sharpening of the sample size distribution reduces the thermodynamic driving force for further growth according to the Ostwald ripening process. As a result, the increase of reaction time (30 min, 1 h) leads to no further increase of the size of tetrapods.

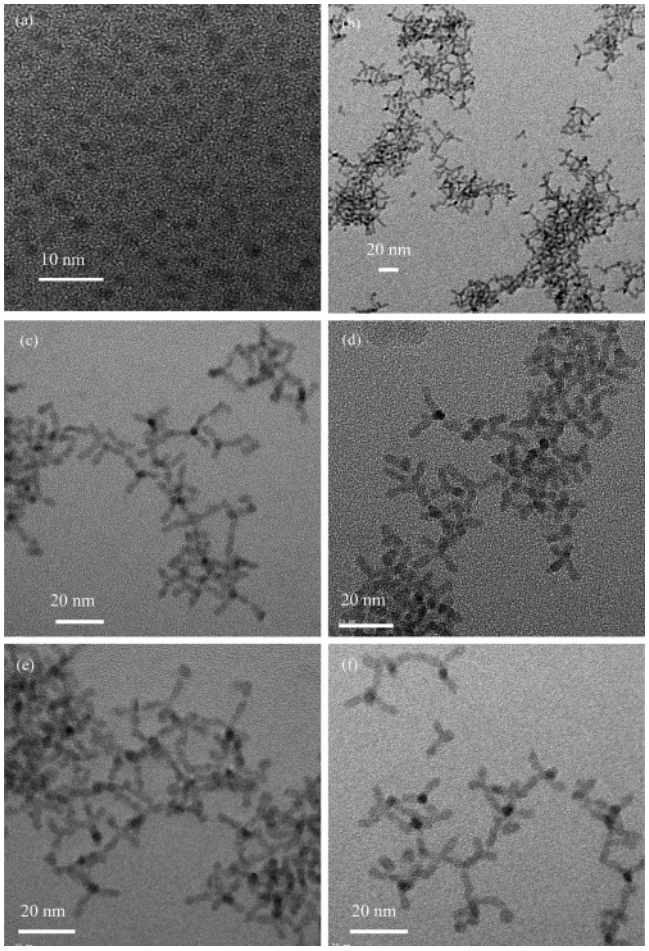

Figure 1. TEM images of (a) sample A, CdSe dots; (b) sample B2, CdSe:HCl (0.6 mmol); (c) sample B3, CdSe:HCl (1.0 mmol); (d) sample C, CdSe:$MnCl_2$; (e) sample D, CdSe:$FeCl_2$; and (f) sample E, CdSe:H_2SO_4.

In our experiment, the only difference between the synthesis of dot-shaped and tetrapod-shaped CdSe nanocrystals is the addition of HCl, H_2SO_4, $MnCl_2$, and $FeCl_2$ into the cadmium precursor separately. The results from the samples with the addition of 0.2 mmol of HCl, 0.6 mmol of HCl, 1 mmol of HCl, and 0.2 mmol of H_2SO_4 suggest that the acidity in the cadmium precursor is responsible for the high yield of CdSe tetrapods. In particular, we planned to synthesize Mn^{2+}- or Fe^{2+}-doped CdSe quantum dots by adding $MnCl_2$ or $FeCl_2$ to the cadmium precursor at first; however, only CdSe tetrapods were obtained. Furthermore, no traces of manganese or iron are detected in the final CdSe tetrapods by EDS in the samples with addition of $MnCl_2$ or $FeCl_2$. This suggests that HCl, H_2SO_4, $MnCl_2$, and $FeCl_2$ are

Table 1. Summary of the Samples' Properties

sample	core diam (size distribution) (nm)	arm length (size distribution) (nm)	arm diam (size distribution) (nm)	PL peak (eV) position	PL peak (eV) fwhm	absorption Peak (eV) lower energy	absorption Peak (eV) high energy
A	4.0 (8%)			2.249	0.120	2.255	2.755
B1	4.0 (7%)	8.1 (12%)	3.0 (8%)	2.141	0.272	2.215	2.716
C	4.2 (7%)	8.5 (10%)	3.3 (9%)	2.123	0.144	2.171	2.659
D	4.1 (9%)	8.5 (15%)	3.1 (9%)	2.204	0.254	2.207	2.690

playing a similar role in the growth of CdSe tetrapods. Noting that the following chemical reactions take place during the reaction process,

$$CdO + 2CH_3(CH_2)_7CH{=}CH(CH_2)_7COOH \rightarrow Cd(CH_3(CH_2)_7CH{=}CH(CH_2)_7COO)_2 + 2H_2O$$

$$MnCl_2 + H_2O \rightarrow Mn(OH)_2 + 2HCl$$

$$FeCl_2 + H_2O \rightarrow Fe(OH)_2 + 2HCl$$

it is clear that the common feature of these additions is proton (H^+) generation from the cadmium precursor. As a result, we believe it is the proton (H^+) that plays a key role in the synthesis of almost pure CdSe tetrapods. $Mn(OH)_2$ and $Fe(OH)_2$ are not soluble under the reaction conditions, which is the main reason doping of CdSe does not take place.

The detailed crystal structure of CdSe tetrapods has been analyzed by HRTEM (see the following paragraph). It is evident that the tetrapod-shaped nanocrystals have a zinc blende core with four wurtzite arms grown out of the four equivalent (111) facets of the zinc blende core, the same as that proposed for CdTe tetrapods.[7] According to previous work, there are two main factors to achieve tetrapod-shaped CdTe and CdSe nanocrystals synthesis. One[7] depends on the growth energy difference between zinc blende and wurtzite structures. At a suitable temperature range one structure could be preferred to another during the synthesis. For the CdTe case, the energy difference between the wurtzite and the zinc blende structures is appropriate for controlling the growth of the zinc blende structure core and wurtzite arms so as to form a tetrapod-shaped nanocrystal easily. However, it has been pointed out that the energy difference between the wurtzite and the zinc blende structures is too small to facilitate controllable tetrapod-shaped nanocrystal synthesis in the case of CdS, CdSe, and ZnS. This is the main reason for a low yield of colloidal CdSe tetrapods.[2,17] On the other hand, it is also reported[2] that the anisotropy nanocrystal growth is determined by the monomer concentration in the solution and a high concentration produces high yield of CdTe nanotetrapods and CdSe nanorods instead of nanotetrapods. In contrast, in our experiments we have found that it is the protonic acidity in the solution that controls the dot-shaped and tetrapod-shaped CdSe nanocrystal synthesis. We believe that the effect of acidic environment in the reaction system is to initiate the growth of the zinc blende core and influence the growth rates of different crystal facets so as to induce anisotropic growth of CdSe nanocrystals. At the beginning of the reaction, the proton (H^+) influences mainly the yield of zinc blende nuclei, and then it may be absorbed on those facets such as {110}, except the four {111} facets, passivating these facets. As a result, the growth can only continue on the four equivalent {111} facets. In the end, the four arms are formed along the unique *C*-axis of the wurtzite crystal. As a surfactant, oleic acid molecules can selectively bind to the other facets of the arms of CdSe, similar to the case of CdTe tetrapod synthesis.[16] Therefore, tetrapod-shaped CdSe nanocrystals can be synthesized in high yield by controlling the protonic acidic circumstance of the reaction solution.

Figure 2a shows the typical HRTEM image of the CdSe tetrapod-shaped structures formed by a core and four arms, which are viewed nearly along the CdSe core [111] direction. Therefore, three arms (labeled by I, II, and III) distribute at an angle of 120° to each other around the core, while the fourth one overlaps with the core. All of the arms have hexagonal structure and are nearly epitaxially connected to the zinc blende CdSe core along the four $\langle 111\rangle_{CdSe}$ directions. The interface structure between the core and arms is $\{111\}_{CdSe}//\{0001\}_{arm}$. From our observations, most CdSe cores have cubic single crystalline structure. However, stacking faults may coexist. In Figure 2a, the HRTEM image of the core shows hexagonal symmetry with a fringe spacing of about 0.37 nm, which is about $\sqrt{3}d_{(220)}$ ($d_{(220)} = 0.212$

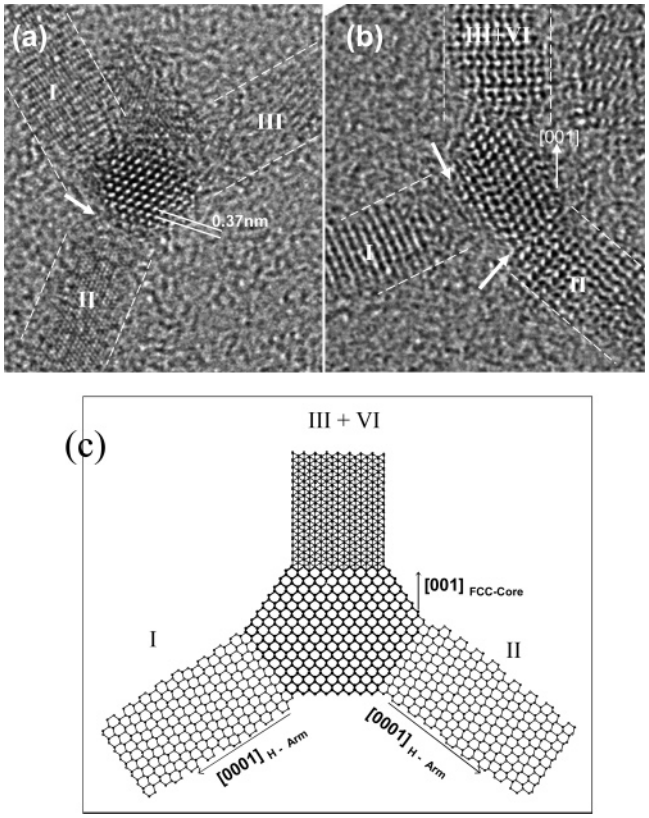

Figure 2. HRTEM images of the tetrahedral structure with one CdSe core particle and four arms: (a) Viewed along the [111] direction of CdSe core particle; (b) viewed along the [110] direction of CdSe core particle; (c) schematic drawing of the tetrahedral nanostructure viewed along the [110] direction of CdSe core particle. The arrows indicate some interface positions between the arms and the CdSe core, and dashed lines are guides for eyes.

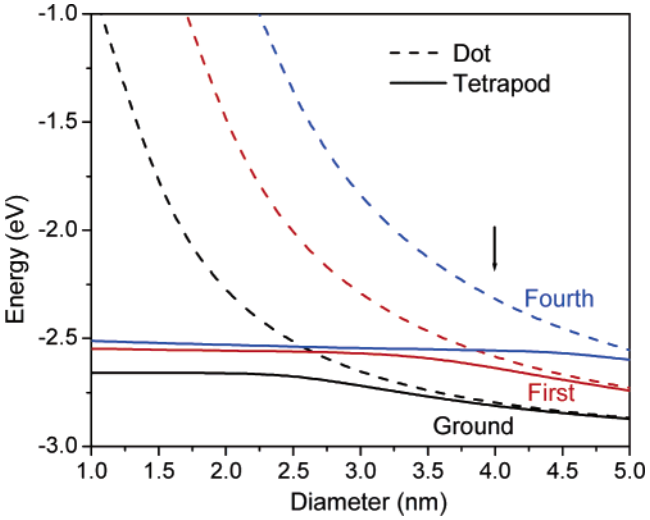

Figure 3. Eigenenergy variation vs core size for dotted (dashed line) and tetrapod (solid line) samples. The arm length and diameter are fixed as 8 and 4 nm. "Ground" refers to the ground state, "First" refers to the first excited state, and so on. The arrow indicates the core size range of our samples.

nm for pure cubic CdSe). Obviously, due to the overlap between the cubic core (viewed in [111]) and the hexagonal arm (viewed in [0001]), the HRTEM image shows two-dimensional moiré fringes with a spacing of about 0.372 nm. This spacing is equal to the $d_{(10\bar{1}0)}$ of the hexagonal arm. The HRTEM image simulations based on this overlapping structure confirm our HRTEM observations. Figure 2b shows the HRTEM image taken along the [110] direction of the core. Arms I and II are typically the hexagonal structure viewed nearly along the $[\bar{1}\bar{1}20]$ orientation, while arms III and IV are overlapped to each other (their $[0\bar{2}23]$ is nearly parallel to the $[110]_{CdSe}$ or the electron beam direction in this figure). Figure 2c shows a schematic drawing of the tetrapod structure viewed along the [110] direction. In this case, overlapping of arms III and IV results in the imaging contrast as shown in Figure 2b. The above analyses confirm the previous proposed structure model for the CdTe tetrapod-shaped nanocrystals.[7]

A one-band envelope function is used to calculate the electronic eigenstates of the CdSe dot and tetrapod. The Hamiltonian used is

$$H = \frac{1}{2m^*}(p_x^2 + p_y^2 + p_z^2) + V(\vec{x}) \qquad (1)$$

where we assume $V(\vec{x}) = -3$eV within the dot or tetrapod and $V(\vec{x}) = 0$ outside the dot or tetrapod; the effective mass of electron $m^* = 0.1\ m_e$ and m_e is the free electron mass.

Figure 3 shows the calculated eigenenergy dependence of the ground state, the first excited state, and the fourth excited state on the diameter of the dot or the core of the tetrapod, respectively. For the tetrapod, the arm dimensions are fixed as 8 nm long and 4 nm wide. The arrow in Figure 3 indicates the core size range of our samples. It can be seen that at smaller core diameters (less than 2.0, 3.0, and 4.5 nm for ground state, first excited state, and fourth excited state, respectively) the eigenenergy of the states is almost unchanged with the decrease of the core diameter. This is because with fixed arm dimensions the wave function

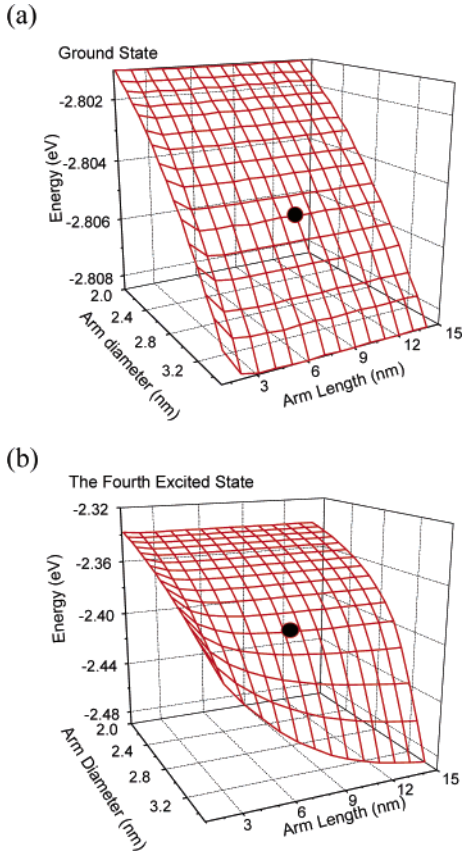

Figure 4. Calculated eigenenergy variation vs the arm diameter and length of a tetrapod with the core size fixed at 4 nm: (a) for the ground state and (b) for the fourth excited state. The black dots indicate the arm sizes of our samples.

distribution within the tetrapod is concentrated inside the arms for smaller core size (armlike states) so that the eigenenergy values are determined mostly by the arm dimensions. As the core diameter increases, the eigenenergy of the tetrapod states becomes closer and closer to that of the dot of the same diameter as the wave function distribution within the tetrapod concentrates more and more inside the core for large enough core size (dotlike states). For our tetrapod samples (indicated by an arrow in Figure 3) the ground state is dotlike, while the fourth excited state is armlike.

Figure 4 shows the ground-state (a) and the fourth-excited-state (b) eigenenergy dependence on the arm diameter and the arm length for the tetrapod. The core diameter is fixed at 4 nm. The black dots in the figure indicate the approximate arm sizes of our tetrapod samples. As can be seen in Figure 4a, the ground-state eigenenergy changes from -2.802 to -2.808 eV when the arm diameter changes from 2.0 to 3.5 nm, but it is almost unchanged when the arm length changes from 3 to 14 nm. This indicates that as the arm diameter increases from 2.0 to 3.5 nm, the eigenenergy decreases only by a few millielectronvolts because the wave function of the ground state is mostly confined inside the core of the tetrapod, i.e., dotlike. On the other hand, the fourth-excited-state eigenenergy (see Figure 4b) decreases more significantly (a few tens of millielectronvolts) with the increase of arm diameter as the wave function penetrates a lot into the arms of the tetrapod, i.e., armlike. For smaller arm diameter (less than about 3 nm) the eigenenergy is almost independent of

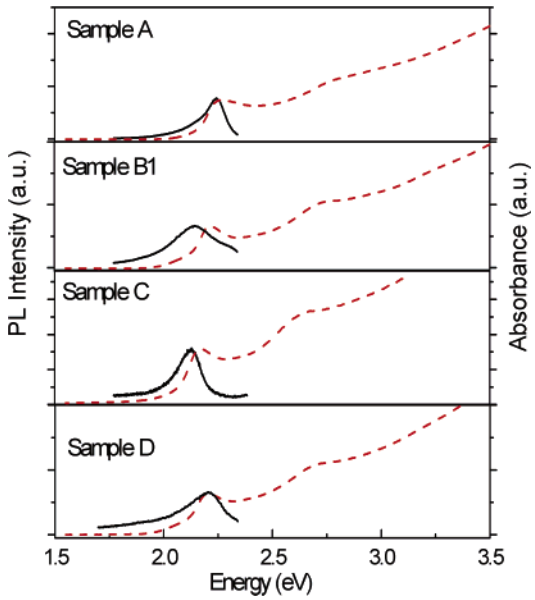

Figure 5. Room-temperature optical absorption (dashed line) and PL (solid line) spectra for samples indicated.

the arm length used here. But when the arm diameter is larger than about 3 nm, the arm length dependence of the eigenenergy is also evident. This is because the quantum confinement of the arm is determined by the aspect ratio of the arm dimension. When the arm diameter is small enough in comparison with its length, the arm resembles a nanowire where the confinement effect is dominated by the arm diameter only. When the arm diameter becomes comparable to its length, both the diameter and length affect the confinement effect. In brief, considering the dimension of our tetrapod samples, the ground state is controlled by the core diameter while the "arm diameter" effect becomes important only for the states above the fourth excited state.

Figure 5 shows the absorption and PL spectra of sample A, B1, C, and D measured at room temperature. No qualitative difference is observed between the dot sample and tetrapod samples as expected from theoretical calculation. The linear absorption spectra of all samples show two peaks. The peak at lower energy originates from the ground-state transition when a 1s electron−heavy hole pair is generated. The higher energy peak is probably a combination of two transitions: one is again a 1s transition that involves the hole from the spin−orbit split-off valence band, and the other is the first excited-state transition. The Stokes shift for the tetrapod sample D is as small as 0.003 eV. The full width at half-maximum (fwhm) of the PL spectrum for the dot sample is narrower than that for the tetrapod samples. The detailed optical properties of the samples are summarized in Table 1.

Conclusion

High yields (about 80%) of tetrapod-shaped CdSe nanocrystals have been successfully synthesized by controlling the acidic circumstance in the OA−TOP reaction system. The core diameter, the arm diameter, and the arm length are estimated to be about 4, 3, and 8 nm, respectively. HRTEM analysis has unambiguously identified that the core of the tetrapod has a zinc blende crystal structure, while the four arms have wurtzite crystal structure. The theoretical calculations indicate that for our tetrapod samples the ground state is dominated by the core diameter and only for the states above the fourth excited state the "arm diameter" effect becomes important. The absorption and PL experiments for the dot and the tetrapod samples show no qualitative difference.

Acknowledgment. J.N.W., S.H.Y., Q.P., and L.J.Z. would like to thank the Research Grant Council of Hong Kong for the financial support via Grant Nos. HKUST6069/02P and F-HK18/03T. The LPA-ENS is "Laboratoire associé au CNRS et aux Universités Paris6 et Paris7" and this work was supported by a Procore Contract (No. 82/222080).

CM050774K